Zeeman interferometric observations of CN(2-1) transitions with CARMA

Manuel Fernández López
Richard Crutcher

Richard Plambeck, Nick Hakobian, Chat Hull,
Leslie Looney & Ian Stephens

Instituto Argentino de
Radioastronomía

I A R
CCT La Plata
CONICET

ISSN: 1853-5461

General Goals

Understanding role of B fields in formation of:

Molecular clouds

Molecular cores

Protostars

Protostellar outflows

Protoplanetary disks

Stars and planets

Theoretical Controversy

Do magnetic fields dominate cloud formation & evolution?

-Strong B models: ambipolar diffusion drives collapse into protostars.
(Mouschouvias 1991; Mouscouvias & Ciolek 1999)

-Weak B models: turbulent flows control cloud formation with cores either dissipating or collapsing if they become self-gravitating.
(Padoan & Nordlund 1999; MacLow & Kleesen 2004)

(Crutcher 2012)

Observational Techniques

Direct measurements:

Zeeman effect

Statistical measurements (Chandrasekhar-Fermi method):

Linearly polarized emission from grains aligned by magnetic fields

Goldreich-Kylafis effect (linear polarization on spectral lines)

Zeeman Effect

Only available technique for measuring directly magnetic field strengths in molecular clouds

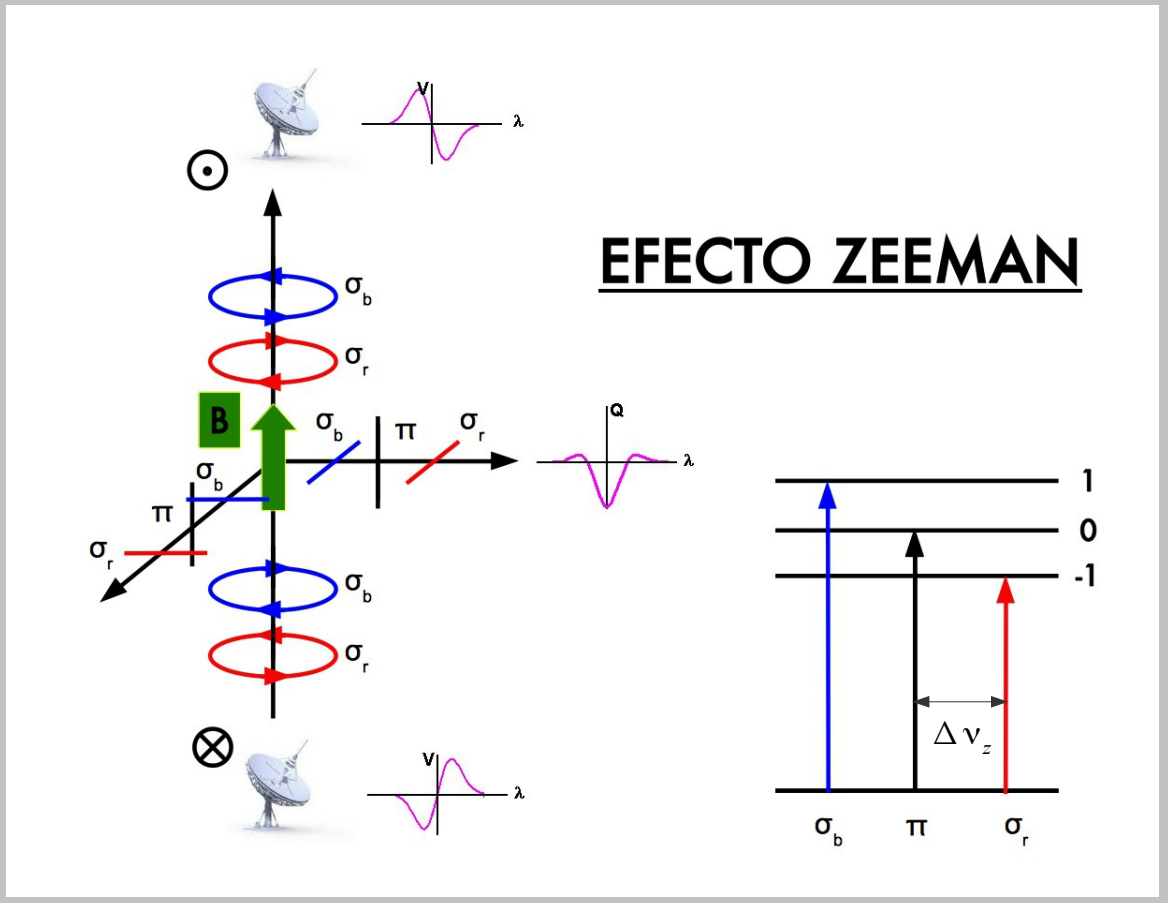

$$V \propto \frac{dI}{d\nu}$$

$$V \propto \frac{\Delta\nu_z}{\delta\nu}$$

$$\Delta\nu_z = \pm Z\, B_{LOS}$$

$$Q, U \propto \left(\frac{\Delta\nu_z}{\delta\nu}\right)^2 B_{POS}$$

Testing Ambipolar Diffusion Model

For Strong B model, M/Φ is expected to increase from envelope to cores

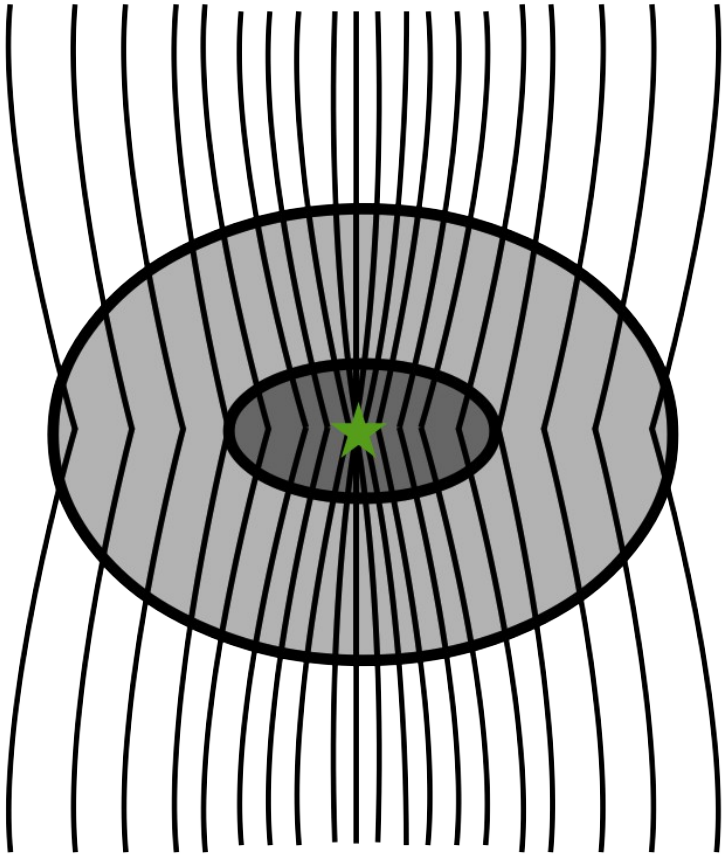

$$M \propto N_{H2}$$

$$\Phi \propto |\vec{B}| \propto B_{LOS} / \cos(\theta)$$

$$\frac{[M/\Phi]_{core}}{[M/\Phi]_{envelope}} = \frac{[N_{H2}/B_{LOS}]_{core}}{[N_{H2}/B_{LOS}]_{envelope}}$$

Massive Star-Forming Sites

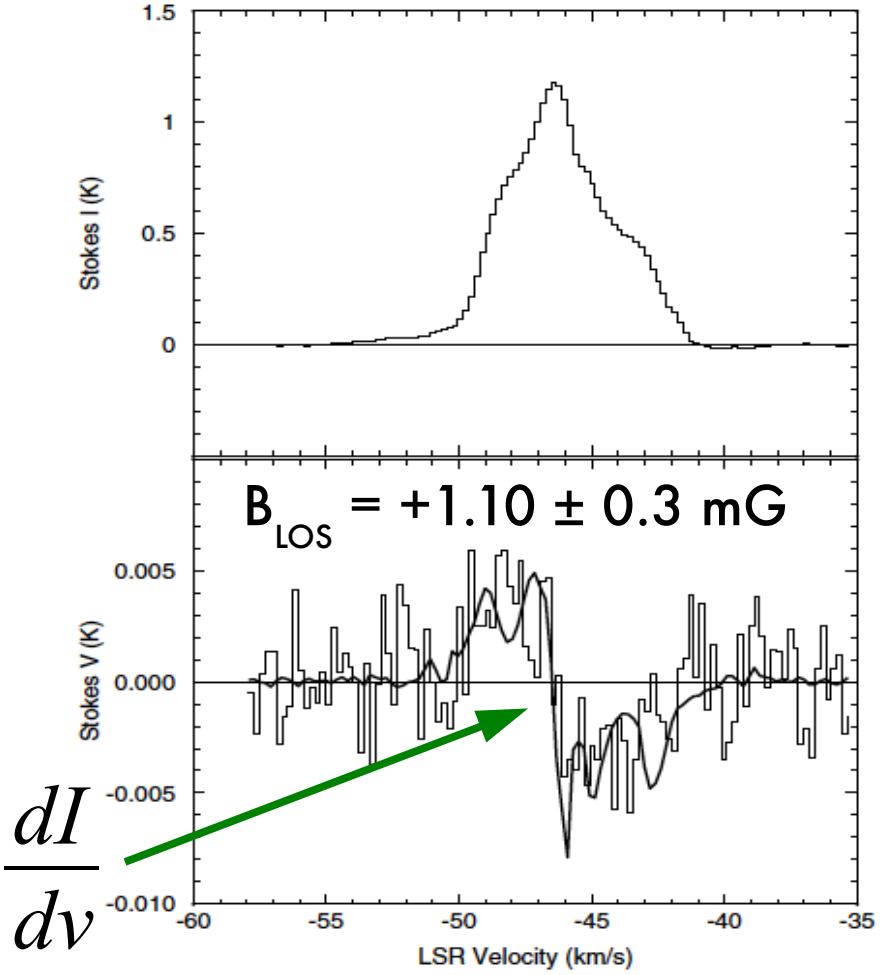

CN Zeeman spectra on W3OH (Falgarone et al. 2008)

CN has a large magnetic dipole, implying larger Zeeman splitting.

CN high density tracer mostly detected in high-mass star-forming regions (DR21 & W3OH).

Single-dish campaigns to detect Zeeman effect in dense clouds using CN.

Crutcher et al. (1996)
Crutcher et al. (1999)
Falgarone et al. (2008)
Maury et al. (2012)

CARMA dataset: 1mm continuum emission

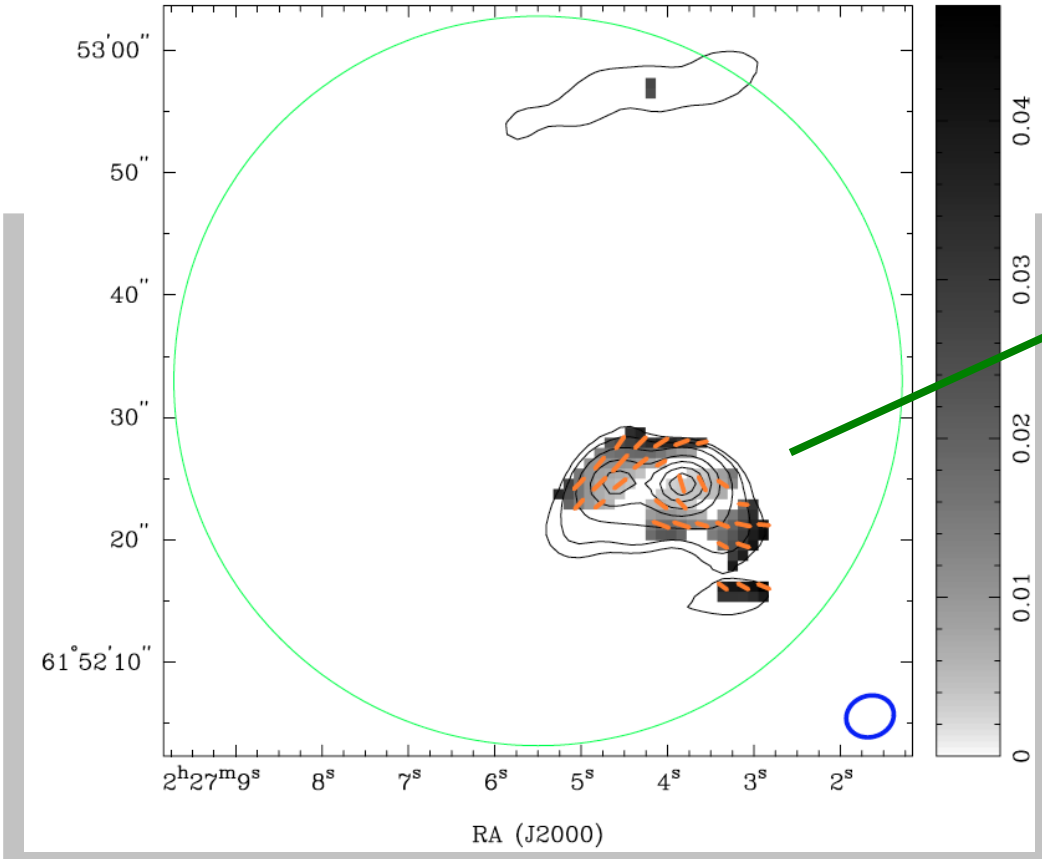

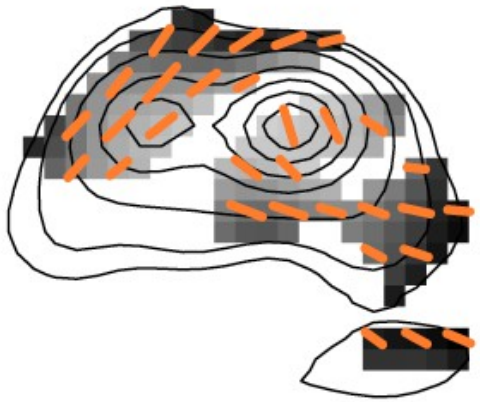

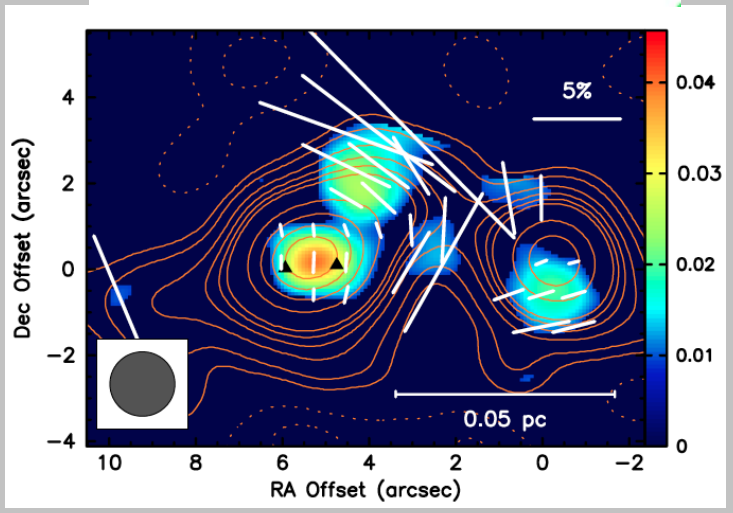

Polarization results similar to those found in Chen et al. 2012 (SMA observations)

CARMA CN(2-1) Observations

Line	$J, F \rightarrow J', F'$	ν (GHz)	Z (Hz/μG)
1	$\frac{3}{2}, \frac{3}{2} \rightarrow \frac{1}{2}, \frac{3}{2}$	226.63217	−0.71
2	$\frac{3}{2}, \frac{5}{2} \rightarrow \frac{1}{2}, \frac{3}{2}$	226.65949	−0.17
3	$\frac{3}{2}, \frac{1}{2} \rightarrow \frac{1}{2}, \frac{1}{2}$	226.66366	−0.61
4	$\frac{3}{2}, \frac{3}{2} \rightarrow \frac{1}{2}, \frac{1}{2}$	226.67934	−1.18
5	$\frac{5}{2}, \frac{5}{2} \rightarrow \frac{3}{2}, \frac{3}{2}$	226.87420	+0.72
6	$\frac{5}{2}, \frac{7}{2} \rightarrow \frac{3}{2}, \frac{5}{2}$	226.87478	+0.40
7	$\frac{5}{2}, \frac{3}{2} \rightarrow \frac{3}{2}, \frac{1}{2}$	226.87591	+1.18
8	$\frac{5}{2}, \frac{3}{2} \rightarrow \frac{3}{2}, \frac{3}{2}$	226.88743	+1.46
9	$\frac{5}{2}, \frac{5}{2} \rightarrow \frac{3}{2}, \frac{5}{2}$	226.89217	+1.05

$$V_i(\nu) = C_1 I_i(\nu) + C_2 \frac{dI_i(\nu)}{d\nu} + C_3 Z_i \frac{dI_i(\nu)}{d\nu}$$

- C1: absorbs gain difference between left and right polarization and any linear polarized line signal.

- C2: absorbs instrumental polarization effects that produce pseudo-Zeeman splitting.

- C3: non-zero if there is circular polarization line splitting due to the CN Zeeman effect.

CARMA CN(2-1) Observations

Fitting 9 CN(2-1) transitions simultaneously

Line	$J, F \rightarrow J', F'$	ν (GHz)	Z (Hz/μG)
1	$\frac{3}{2}, \frac{3}{2} \rightarrow \frac{1}{2}, \frac{3}{2}$	226.63217	−0.71
2	$\frac{3}{2}, \frac{5}{2} \rightarrow \frac{1}{2}, \frac{3}{2}$	226.65949	−0.17
3	$\frac{3}{2}, \frac{1}{2} \rightarrow \frac{1}{2}, \frac{1}{2}$	226.66366	−0.61
4	$\frac{3}{2}, \frac{3}{2} \rightarrow \frac{1}{2}, \frac{1}{2}$	226.67934	−1.18
5	$\frac{5}{2}, \frac{5}{2} \rightarrow \frac{3}{2}, \frac{3}{2}$	226.87420	+0.72
6	$\frac{5}{2}, \frac{7}{2} \rightarrow \frac{3}{2}, \frac{5}{2}$	226.87478	+0.40
7	$\frac{5}{2}, \frac{3}{2} \rightarrow \frac{3}{2}, \frac{1}{2}$	226.87591	+1.18
8	$\frac{5}{2}, \frac{3}{2} \rightarrow \frac{3}{2}, \frac{3}{2}$	226.88743	+1.46
9	$\frac{5}{2}, \frac{5}{2} \rightarrow \frac{3}{2}, \frac{5}{2}$	226.89217	+1.05

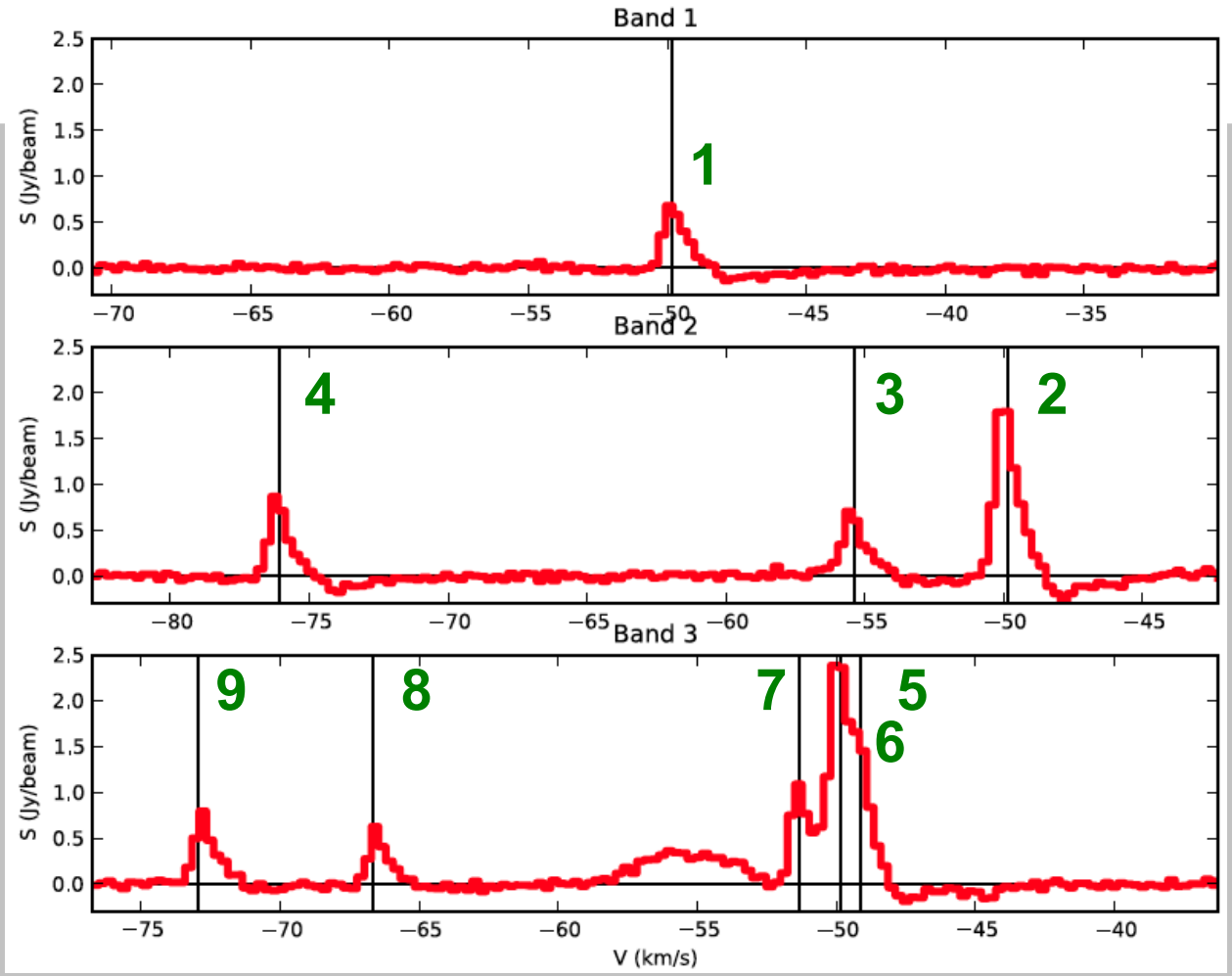

Observed Spectral Bands

Zeeman effect detections

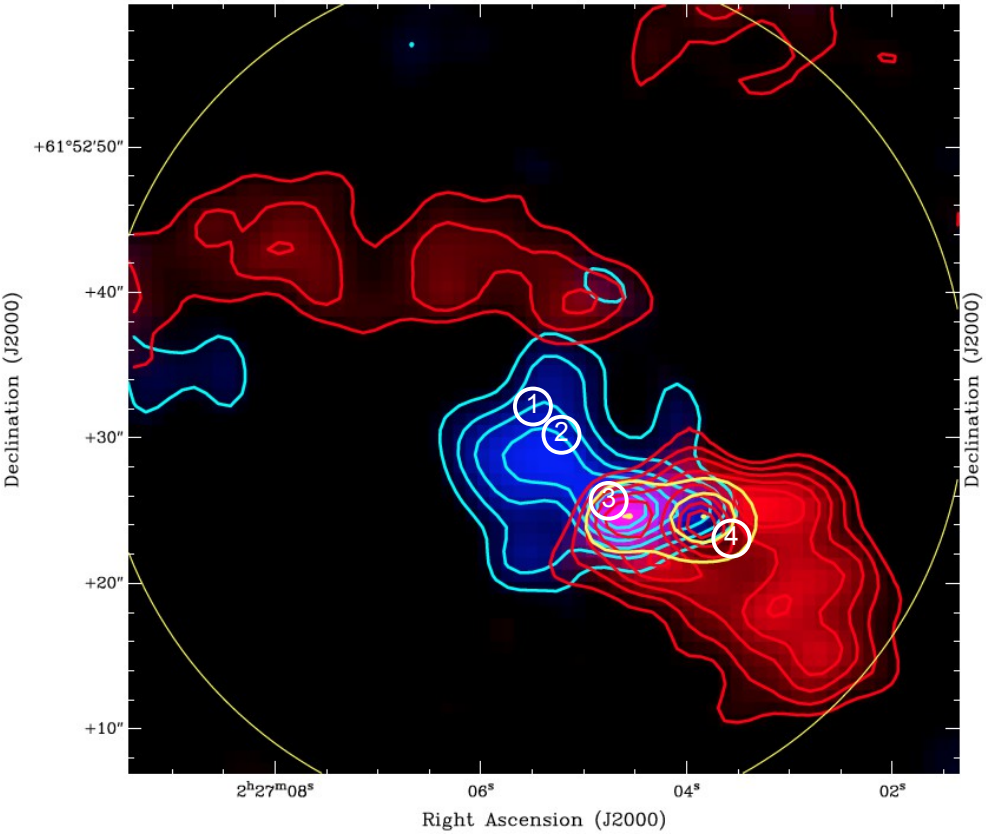

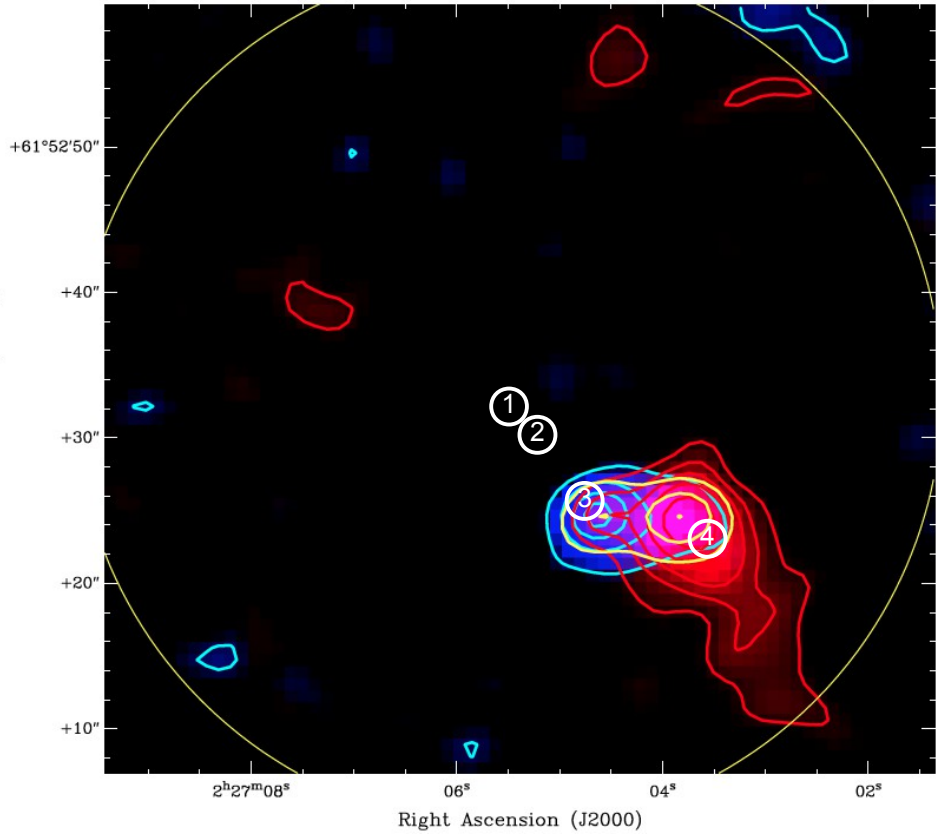

Low velocity gas

|V| c [0.3,4.5] km/s

High velocity gas

|V| c [4.5,10.0] km/s

Zeeman effect detections

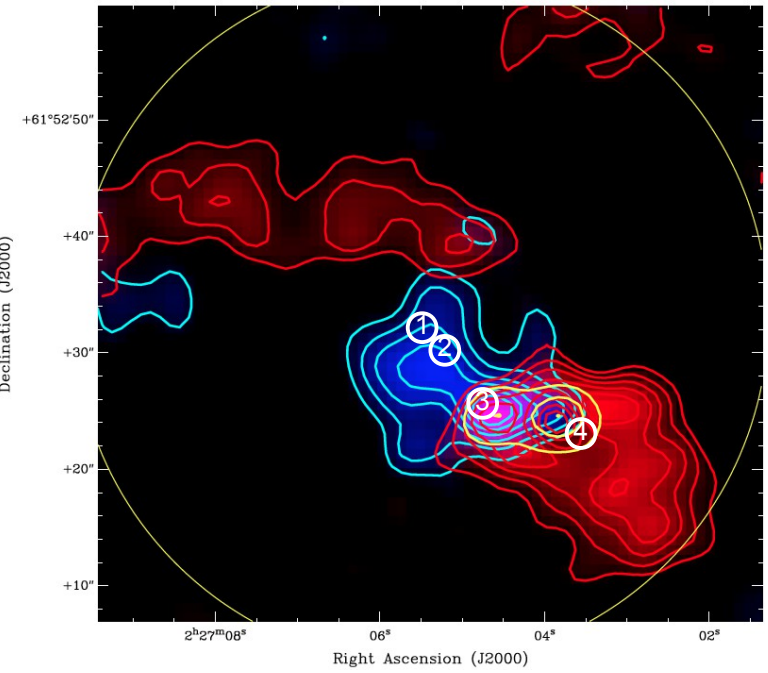

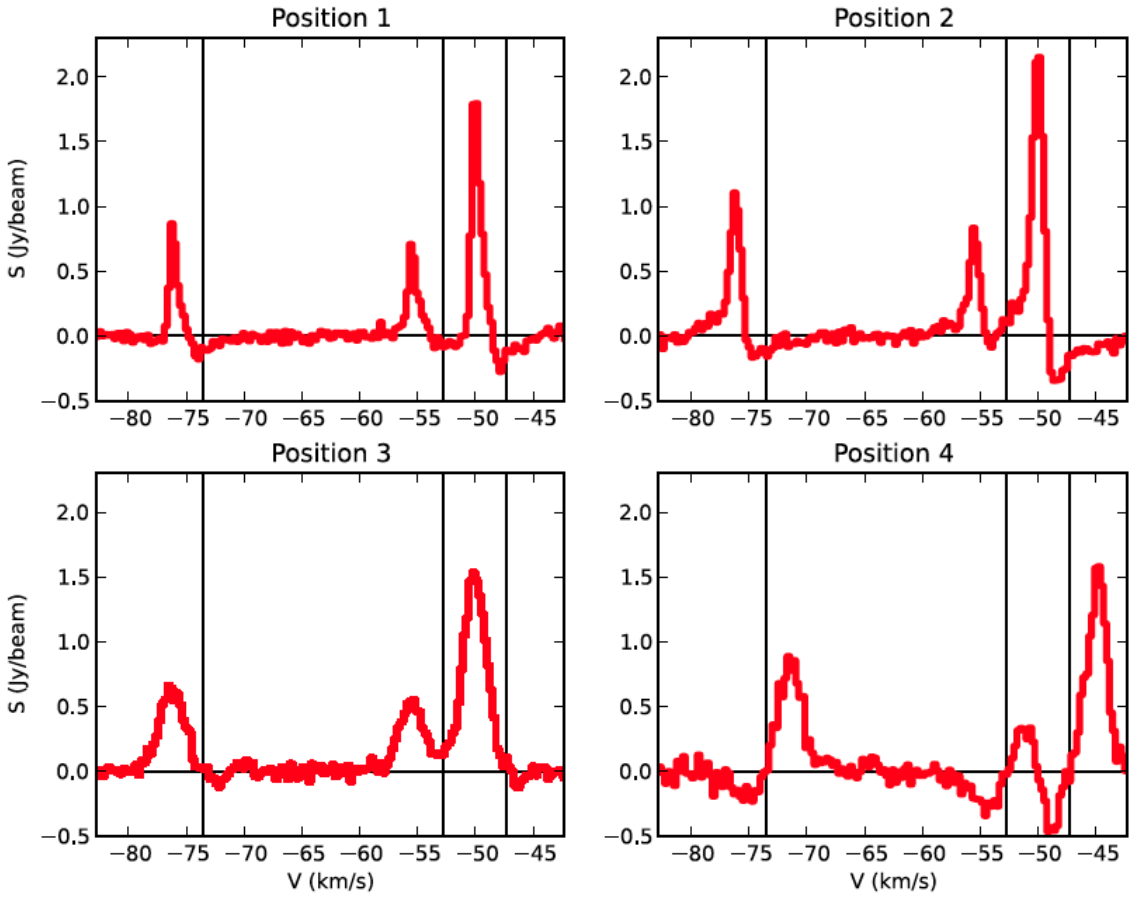

- Selected positions with “easy” spectra.

- Zeeman effect detected through the analysis of the 9 spectral lines simultaneously.

Zeeman effect detections

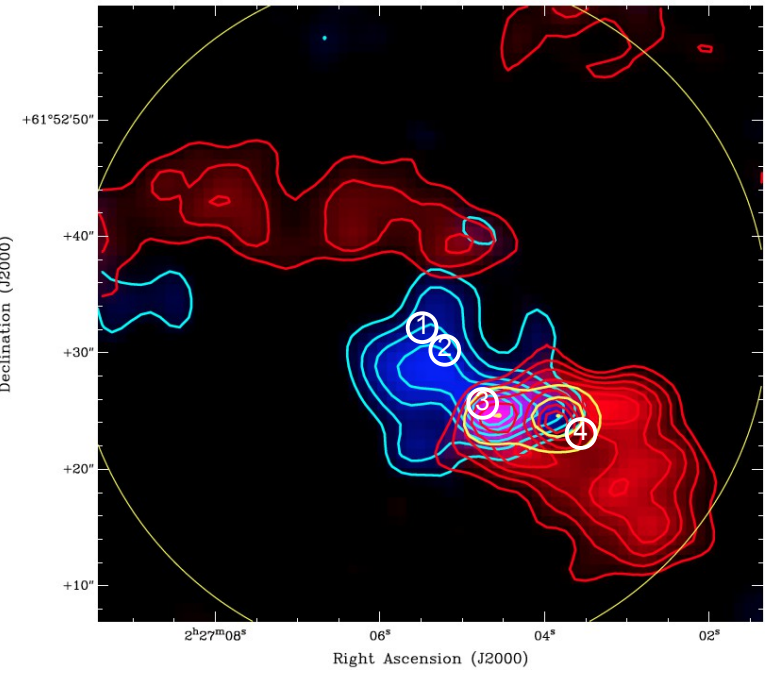

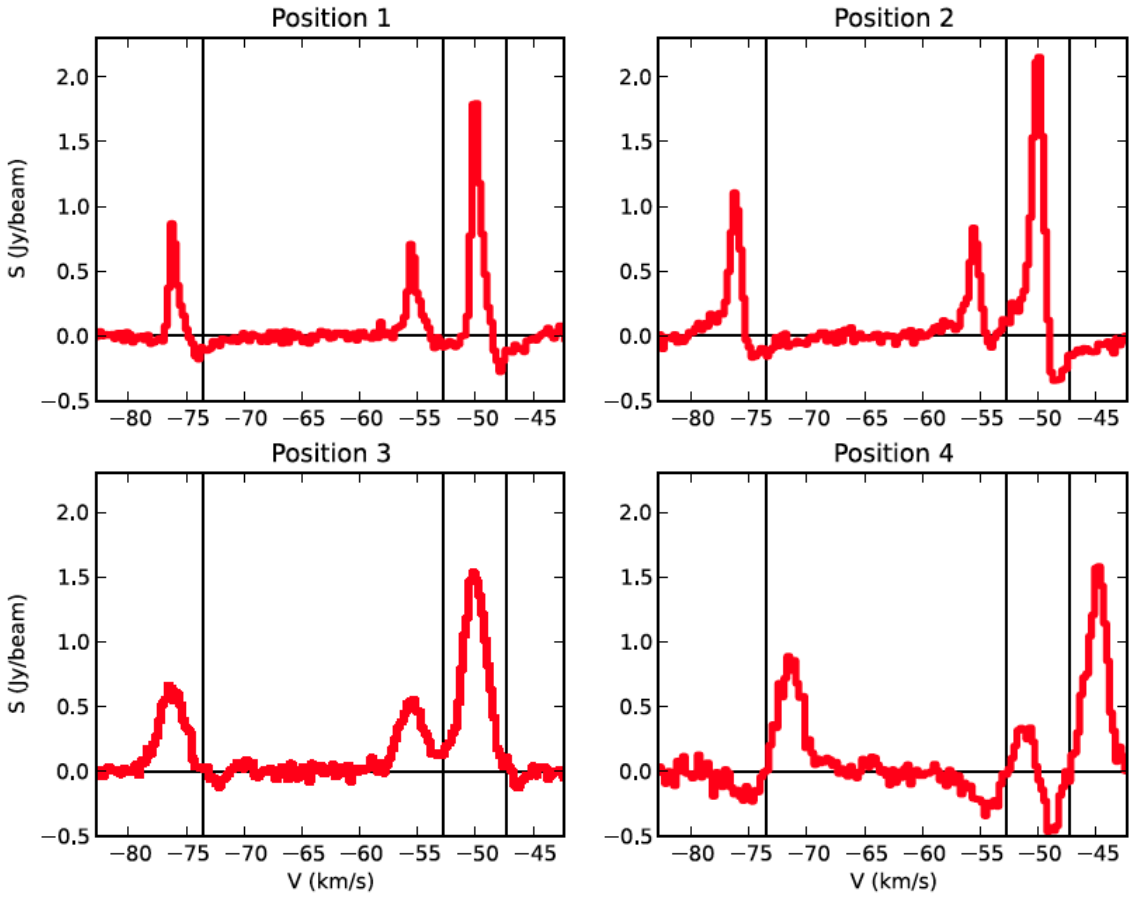

Position	Blos (mG)
1	+4.5 ± 1.1
2	+4.2 ± 1.3
3	-2.4 ± 1.7
4	-2.0 ± 1.1

First detection of Zeeman effect with an interferometer!

CONCLUSIONS

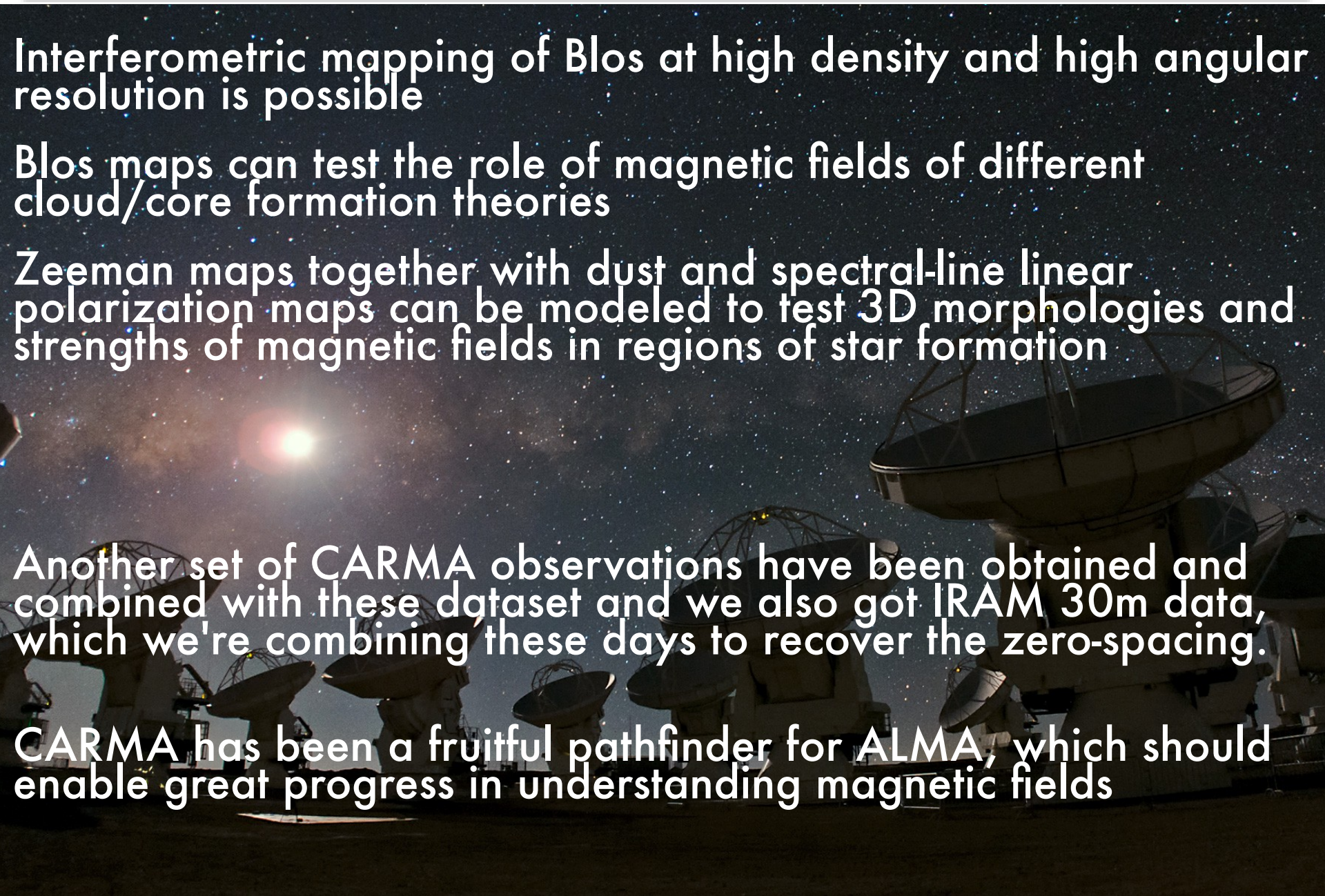

Interferometric mapping of Blos at high density and high angular resolution is possible

Blos maps can test the role of magnetic fields of different cloud/core formation theories

Zeeman maps together with dust and spectral-line linear polarization maps can be modeled to test 3D morphologies and strengths of magnetic fields in regions of star formation

Another set of CARMA observations have been obtained and combined with these dataset and we also got IRAM 30m data, which we're combining these days to recover the zero-spacing.

CARMA has been a fruitful pathfinder for ALMA, which should enable great progress in understanding magnetic fields

MUCHAS GRACIAS

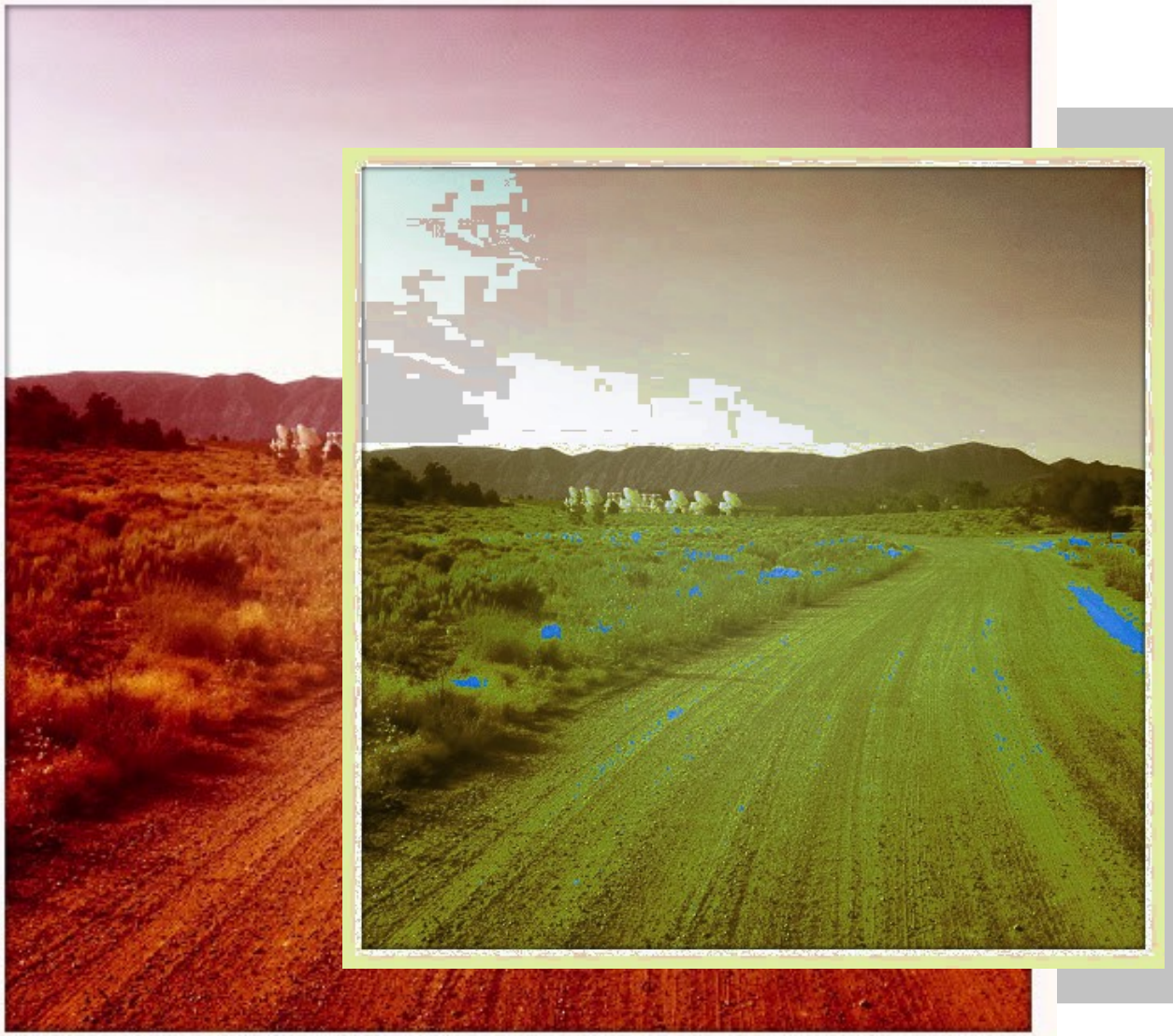

CARMA telescope. Cedar Flat, Big Pine, CA.

Hints of G-K effect detection

Velocity INTEGRATED EMISSION maps
&&
Velocity AVERAGED linearly POLARIZED emission

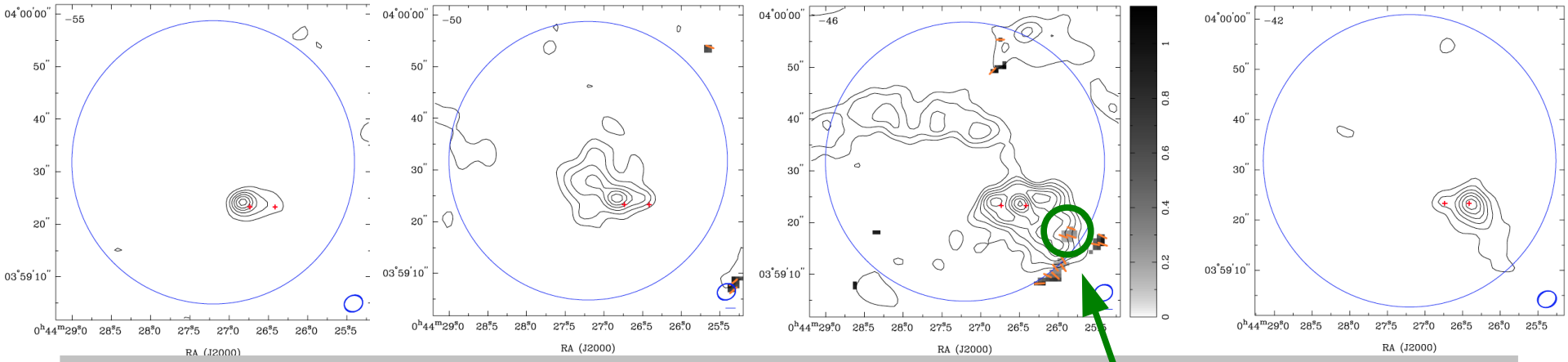

- Hints of G-K effect (linearly polarized CN emission).
- We have to add the rest of the lines.

Hints of G-K effect detection

Velocity INTEGRATED EMISSION maps
&&
Velocity AVERAGED linearly POLARIZED emission

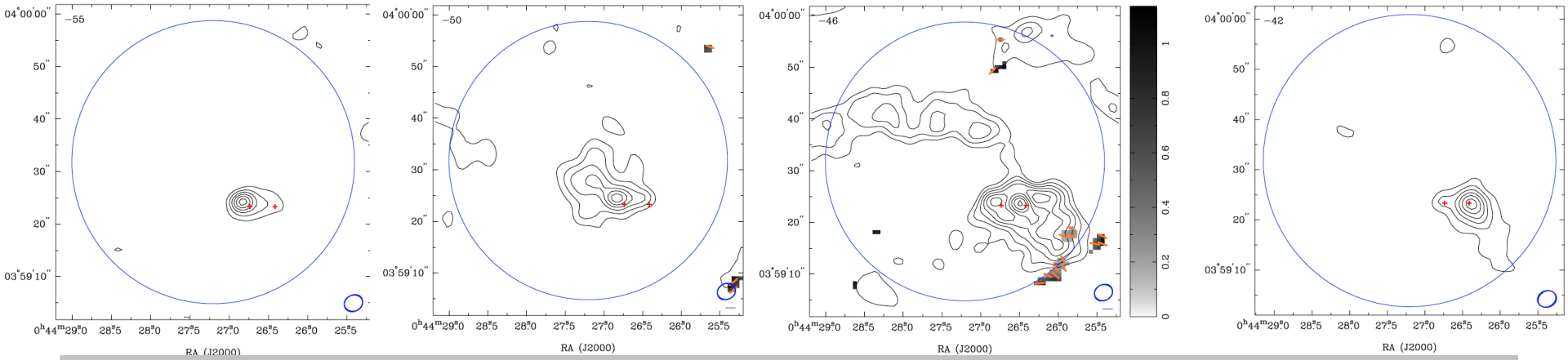

Hints of G-K effect detection